Hindawi
Adsorption Science & Technology
Volume 2023, Article ID 4126562, 11 pages
https://doi.org/10.1155/2023/4126562

Research Article

An Economical Modification Method for MIL-101 to Capture Radioiodine Gaseous: Adsorption Properties and Enhancement Mechanism

Peng Wang,[1,2] **Bing-Bing Qi**,[1] **Ao-Tian Gu**,[1] **Kai-Wei Chen**,[1] **Chun-Hui Gong**,[1] **and Yang Yi**[1]

[1]*Jiangsu Key Laboratory of Chemical Pollution Control and Resources Reuse, School of Environmental and Biological Engineering, Nanjing University of Science and Technology, Nanjing 210094, China*
[2]*Key Laboratory of Nuclear Technology Application and Radiation Protection in Astronautics (Nanjing University of Aeronautics and Astronautics), Ministry of Industry and Information Technology, China*

Correspondence should be addressed to Chun-Hui Gong; gongchunhui@njust.edu.cn and Yang Yi; yangyi@njust.edu.cn

Received 3 October 2022; Revised 27 November 2022; Accepted 8 December 2022; Published 27 March 2023

Academic Editor: Chinenye Adaobi Igwegbe

Radioactive iodine is one of the inevitable by-products of nuclear energy application. However, it is a great threat to public health and the adsorbent needs to be adopted for removing the radioactive iodine. The iodine adsorbent needs to have some advantages, such as simple preparation method, low cost, high absorption capacity, and recyclable utilization. In order to meet the above requirements, the etched material of institute Lavoisier 101 (MIL-101) was prepared to absorb the gaseous iodine. After the MIL-101 is etched, the iodine adsorption performance has been greatly improved. The iodine adsorption experiment of etched MIL-101 with different etching time (1 h, 3 h, 4 h, and 6 h) was completed, the results show that the optimal etching time is 4 hours and the capture capacity of the etched MIL-101 is 371 wt%, which is about 22% higher than that of original MIL-101. The experiment results of XRD, FT-IR, and XPS prove that the components and structure of etched MIL-101 are accordable with those of MIL-101. The surface roughness is introduced in this work. The pore roughness is also an important factor to the adsorption capacity, and the related research also supports this conclusion. Furthermore, after iodine is absorbed, etched MIL-101 can be treated by ethanol for iodine release, and the etched MIL-101 has satisfied recyclability within three cycles. Compared with MIL-101, etched MIL-101 not only had good reversible adsorption of iodine but also can adsorb low-concentration iodine. The etched MIL-101 has a broad application prospect in nuclear emergency response and radiation detection.

1. Introduction

With the development of nuclear technology, the public health threat of artificial radionuclide gradually increases. Especially radioactive iodine, it has attracted great attention in the application of nuclear energy and nuclear technology [1]. Radioactive iodine usually exists in the form of iodine, which is easily diffused. It will enter the human body through various media such as air, water, and food, and then it is rapidly enriched by the human thyroid gland, thereby causing various thyroid diseases [2]. Currently, there are 37 known types of iodine isotope and their mass numbers are ranging from 108 to 144.15 types of radioiodine are produced by nuclear power plant. However, the ^{129}I and the ^{131}I are the two most harmful to the humans and the environment. The half-life of ^{129}I is 1.57×10^7 years [3]. Therefore, the ^{129}I will cause continuous pollution to the

ecosystem. The amount of release ^{131}I is huge, hundreds of times higher than released other radionuclides [4]. In order to prevent radioiodine damage to humans and the environment, it needs to be enriched. Adsorption material is considered to be one of the most promising methods for radioiodine removal [5]. Therefore, it is a challenge to develop recycled adsorbents with high adsorption capacity, low cost, and high stabilities [6].

In the world, some types of material actually have been applied to the radioiodine adsorption, such as the activated carbon and functionalized clay. However, these materials do not have enough adsorption capacity [7].

The adsorbent with silver has been considered as the best choice for radioactive iodine adsorption, and the reaction mechanism is that silver and iodine were used to produce silver iodide [8, 9]. Compared with activated carbon and other traditional adsorbent, the silver containing material has excellent adsorption performance. However, the high cost and nonrecycling silver-based adsorbent hinder its wide application.

The conjugated microporous polymers (CMPs) and covalent organic frameworks have excellent gas adsorption property and they have great potential in iodine adsorption [10, 11]. However, the preparation of materials is complicated and material synthesis is sensitive to temperature, pressure, and reaction atmosphere. In addition, ligands used in synthetic materials are difficult to obtain and expensive. Therefore, the preparation process of material needs further development.

The metal-organic frameworks (MOFs) have become one of the potential adsorption materials for radioiodine due to amounts of active adsorption sites, a high specific area, and high porosity [12–14]. The MOFs are a kind of porous material composed of organic ligands with metal ions or metal clusters [15]. MOFs are also ideal materials for gas storage and separation [16–20]. The preparation method of MOFs is very simple and suitable for industrial large-scale production, such as ZIF-8 and MIL-101. The zeolitic imidazolate framework-8 (ZIF-8) had been prepared to capture radioactive iodine [21]. The ZIF-8 contained six-membered-ring apertures with diameters of 3.4 Å, which is close to the diameter of iodine molecules (3.35 Å). The adsorption capacity of ZIF-8 is 125 wt% for iodine vapor; only 25% of the iodine was absorbed on the surface and 100% of the iodine was captured in the structure. However, iodine can escape from the inside of ZIF-8 at 300°C, and it has cyclic adsorption properties [22]. In addition to the ZIF-8, the MIL-101 is also a kind of excellent MOFs material. French scientist Ferey prepared MIL-101 in 2005, and the MIL-101 has been widely used in catalysts, gas adsorption, sensors, and other fields [23]. The MIL-101 is formed by the chromium ions and terephthalic acid. Due to high specific area, excellent chemical and thermal stability, MIL-101 is considered as one of the most promising iodine-adsorbent materials [24]. Furthermore, MIL-101 could capture iodine (96.61%) at a faster kinetics.

Currently, more and more kinds of modified MIL-101 materials have been studied. There are two pathways to increase the adsorption capacity of MIL-101, one of which is to improve the porosity and the other is increasing the adsorption point. Ahmed et al. prepared GO/MIL-101 composite material with high porosity. A small amount of graphene can improve the porosity of composite. However, as the amount of GO increases, the porosity of composite begins to decrease. The adsorption capacity of GO/MIL-101 for nitrogen containing compound (NCC) is far more than MIL-101 [25]. Zhou et al. synthesized bimetallic MIL-101 (Cr, Mg). Due to the increased specific area of MIL-101, the adsorption capacity of CO_2 was significantly improved and reaching 3.28 mmol/g for CO_2 [26].

Montazerolghaem et al. successfully manufactured Cu@MIL-101 and Ni@MIL-101 and studied the adsorption properties of Cu@MIL-101 and Ni@MIL-101 for CO_2. The Ni nanoparticles are uniform in MIL-101 distribution than Cu due to smaller size. Thus, Ni@MIL-101 absorbs CO_2 better than Cu@MIL-101 [27]. The adsorption properties of a series of MIL-101 with different anions (Cl^-, F^-, and NO_3^-) to N_2, H_2, and CH_4 have been studied by Berdonosova et al. [28]. The results show that the Cl^- doped MIL-101 has higher gas adsorption properties than the other anion-modified materials.

The modified MIL-101 should have better performance but modification process cannot be too complicated and the cost of the modification reagents cannot be too high. The etching method is a suitable modification method [29]. To improve the absorption capacity and simplify preparation method, the etched MIL-101 is thoroughly studied as iodine adsorbent. The etched MIL-101 has some advantages of simple preparation method, low cost, high absorption capacity, and recyclable utilization. In this study, the enhancement effect and mechanism for etching process are deeply discussed. Through the research for adsorption capacity of MIL-101 with different etching time, the importance of the pore surface roughness was found. This conclusion is further confirmed by comparing the results of previous studies. The specific surface area, pore roughness, and adsorption site collectively influence the absorption capacity of MOFs.

2. Experiments and Methods

2.1. Chemicals and Material. The chemicals including terephthalic acid (H_2BDC), chromic nitrate nonahydrate ($Cr(NO_3)_3 \bullet 9H_2O$), hydrofluoric acid (HF), deionized water (H_2O), iodine (I_2), N,N-dimethyl formamide (DMF), ethanol(C_2H_6O), and glacial acetic acid ($C_2H_4O_2$) were purchased commercially. All reagents were of analytical grade, which were used without further purification.

2.2. Synthesis of Etched MIL-101. The MIL-101 was manufactured according to the hydrothermal method [29], as shown Figure 1. 4.00 g $Cr(NO)_3 \bullet 9H_2O$ and 1.66 g H_2BDC were weighed on by an electronic balance (METTLER TOLEDO AL-104). These reagents and 50 mL deionized water were added in a 100 mL beaker, and whisked it at room temperature until dissolved. 12 mL HF was poured into the solution. Then, the mixture was ultrasonic shaking for 15 min and transferred to a 100 mL Teflon liner of

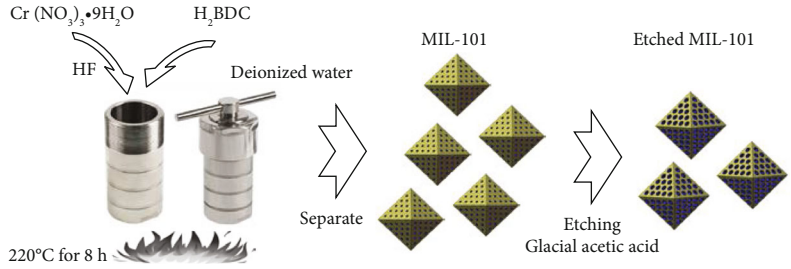

Figure 1: Schematic diagram of preparation process of the etched MIL-101.

high-pressure reactor. After the reactor was fully tightened, it was placed in an electric blast drying over (JingHong DHG90A) at 220°C for 8 h. The produced precipitate was separated and dried in vacuum at 100°C overnight (SuoPu DZF-6050). The MIL-101 was successfully prepared.

The 400 mg of MIL-101, 50 mL of deionized water, and 5 mL of glacial acetic acid were placed in a 100 mL of reactor, and stir quickly for 5 min to disperse MIL-101 evenly. Then, the reactor was moved to the drying incubator in 180°C for a period of time. When the reactor is cooled to room temperature, the mixture was centrifuged, and the etched MIL-101 was achieved [30].

2.3. Characterization. The crystallized phases of powder were recorded by X-ray diffraction (XRD), and the measuring instrument was D8 ADVANCE of Bruker (Cu Kα radiation). The micromorphology and nanostructure were shown by scanning electron microscopy (SEM, FEI Quant 250FEG, USA) and transmission electron microscope (TEM, FEI Tecnai 20, USA). The test condition of SEM was 30 kV and the sample needed to be treated by gold sputtering. Thermogravimetric analysis (TGA) was used to thermal stability in air with a heating rate of 10°C min^{-1} and the temperature range is from 50 to 800°C. The infrared spectra (IR) spectroscopy was obtained on a spectrometer meter by using KBr pellets (Bruker VERTEX 70). The Brunauer-Emmett-Teller (BET, Gold-APP V-Sorb2800P, China) specific area and pore size distribution were measured based on the nitrogen adsorption/desorption analyses using surface area analyzer. Samples were vacuum desorbed at 160°C for 12 h and then the material was tested at 77 k for BET. The XPS spectra were measured by using a PHI Quantera II electron spectrometer with a monochromatic Al Kα radiation.

2.4. Adsorption Experiment. In order to determine the iodide adsorption properties of samples, the capture experiment of iodine was adsorption of gaseous iodine. Considering the high harmfulness of radioactive iodine, the iodide experiments were performed with nonradioactive ^{127}I as alternative. The nonradioactive ^{127}I is no harm to the experimenter's health. In addition, the radioactive ^{131}I, ^{129}I, and nonradioactive ^{127}I have the same physicochemical performance for absorption experiments [4–6].

In the gaseous iodine capture experiment, the 20 mg of adsorption material was placed in a sealed container with solid iodine at 350 K and the normal pressure. The quality of the solid iodine is 10, 50, 100, 200, 300, 400, and 500 mg. After 8 h of adsorption, the container was opened quickly in the draught cupboard for releasing the unabsorbed gaseous iodine. The mass of adsorption material was weighed by the analytical balance after cooling down to room temperature. The adsorption amount of iodine was calculated based on the mass difference before and after the capture. The calculation equation is shown as follows:

$$\frac{m_2 - m_1}{m_1} \times 100\,\text{wt\%}, \quad (1)$$

where m_1 and m_2 are the mass of sample before and after adsorption, respectively [31].

The procedure of iodine desorption is simple. Because I_2 is soluble in organic solvents, such as ethanol, cyclohexane ,and acetone, the iodine desorption experiment can be completed by ethanol washing. The adsorbed sample was placed in 10 mL ethanol for 8 h, then they were dried for 12 h in vacuum at 160°C.

3. Results and Discussions

3.1. Characterization. The morphology of the MIL-101 and the etched MIL-101 were monitored using a SEM. As presented in Figure 2(a), original MIL-101 showed a well-defined octahedron shape structure with particle sizes of ~400 nm and smooth surface. However, the surface of etched MIL-101 became slightly rough; as the Figure 2(b) shows, and the shape and size of the material did not change anything. From the outer surface of the material, it can be inferred that the inside of the pore also becomes very rough. Some etched MIL-101 crystals were found that the hollow structure was formed in the interior of the material, and the inner surface of the pore is very rough, as shown in Figure 2(c).

XRD pattern of etched MIL-101 and MIL-101 is shown in Figure 3. The main characteristic peaks of MIL-101 appeared at 5.24°, 8.52°, and 9.13°, it is indicated that the material was MIL-101 [32, 33]. Compared with the XRD pattern of the MIL-101 that of etched MIL-101 does not appear new characteristic peaks and just a slight change in intensity for characteristic peaks. XRD patterns demonstrate that the etching process has no effect on the crystal structure of MIL-101. That is to say that the etched MIL-101 has the same crystal structure as the MIL-101.

FT-IR spectrograms studies of the original MIL-101 and etched MIL-101 have been performed and shown in

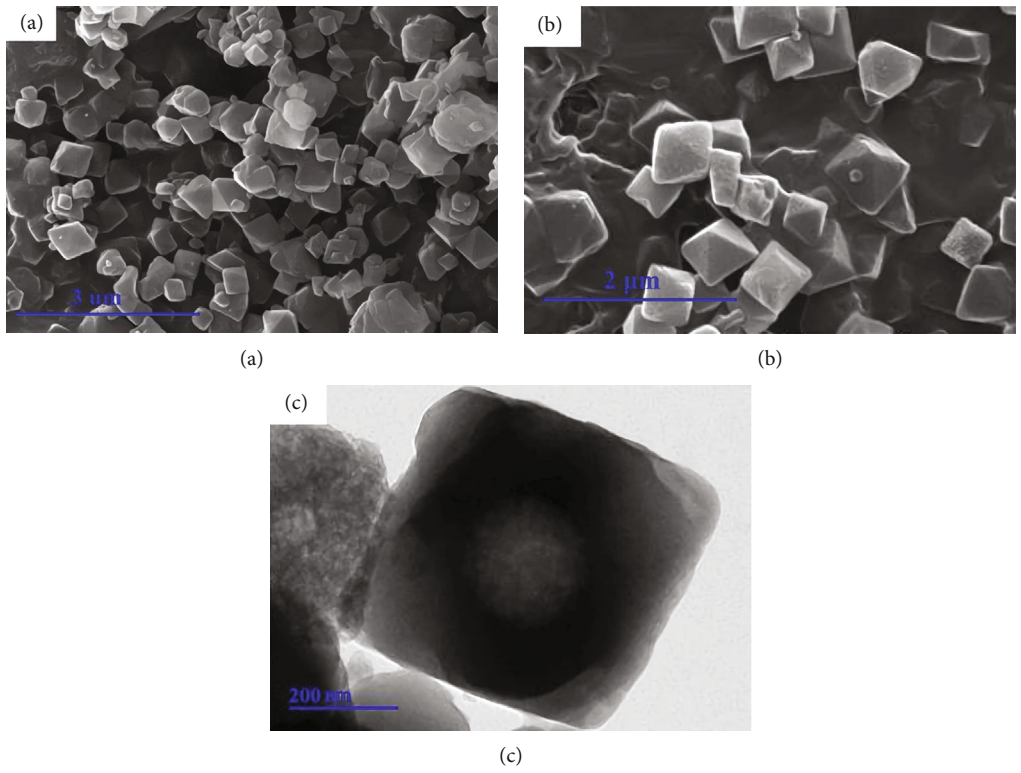

Figure 2: (a) The SEM photograph of the MIL-101. (b) The SEM photograph of the etched MIL-101. (c) The TEM photograph of the etched MIL-101.

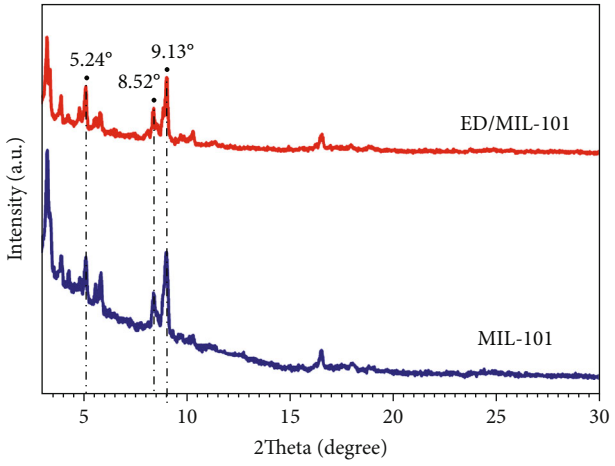

Figure 3: The XRD results of etched MIL-101 and MIL-101.

Figure 4(a). The FT-IR spectra for the material were recorded in the range of 2000-500 cm^{-1} that displayed a range of vibrational and binding modes. As depicted in Figure 4(a), the absorption peaks at 1630 cm^{-1} and 1530 cm^{-1} should be attributed to the C=C and the aromatic ring [34, 35]. The peak absorbance at 1420 cm^{-1} corresponds to the telescopic vibration of the C-O. The characteristic peaks of 1000-1250 cm^{-1} were generated by the chemical single bonds, such as C-O, C-N, and C-F, and these peaks were significantly attenuated. The results show that the etching process damages a portion of bonds.

In contrast with the FT-IR spectrograms of MIL-101, the characteristic peaks of MIL-101 did not significantly change in the FT-IR spectrograms of etched MIL-101, and no new characteristic absorption peaks appeared. It indicates that the etching process does not change the structure of the matrix material MIL-101.

Figure 4(b) is the TGA result of original MIL-101 and etched MIL-101 in air. It is well depicted that etched MIL-101 has a similar thermal stability to the original MIL-101. There are three obvious weightlessness processes in the TGA curves. The first weightlessness processes occurred at 50-100°C, mainly the water attached to the surface of the material was evaporated in air. The second weightlessness processes happened at 100-300°C, the primary reason was a loss of water molecules and small molecules in the pore. The third falling with the range of 300-350°C corresponded to the elimination of OH/F groups and decomposition of the framework. The TGA curve indicates that the etching processes does not change the MIL-101 structure.

As shown in Table 1, the nitrogen adsorption-desorption isotherms were measured to investigate the effect of different etching times on porosity. The specific area and pore volume of MIL-101 were calculated to be 3134 m^2g^{-1} and 1.52 cm^3g^{-1}, respectively. However, etching process changes the specific area and pore volume, and the specific area of the etched MIL-101 is decreased continuously with the increasing etching time. In addition, the pore volume is increased continuously with the increasing etching time. The curves of pore size distribution were displayed in Figure 5(a), and pore size was increased continuously with the increasing etching time. That

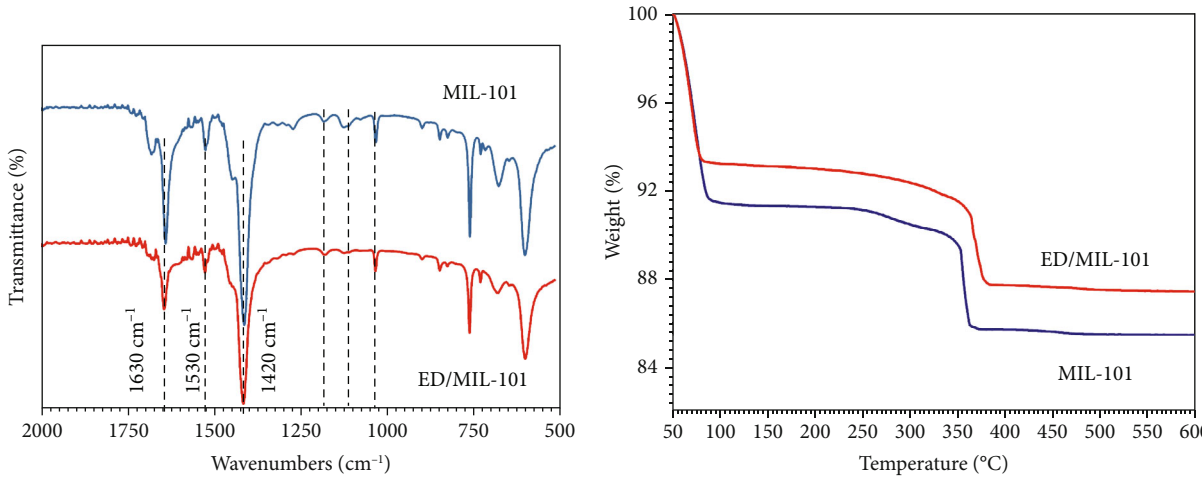

Figure 4: (a) FT-IR spectrograms of MIL-101 and etched MIL-101. (b) The TGA curves of MIL-101 and etched MIL-101.

Table 1: The specific area and pore volume of etched MIL-101.

Adsorbent	Specific area (m^2/g)	Pore volume (cm^3/g)	Pore size (nm)
MIL-101	3134	1.52	2.23
1 h etched MIL-101	3071	1.53	2.23
3 h etched MIL-101	2902	1.58	2.23
4 h etched MIL-101	2753	1.62	2.27
6 h etched MIL-101	2524	1.67	2.29

means the surface of the pore is corroded away; however, the structure of the pore does not collapse. The SEM images showed that the outer surface of the material became very rough, combined with the aperture change, the internal surface of the pore should be very rough.

As shown in Figure 5(b), the curves of nitrogen adsorption-desorption isotherms of and different etching time MIL-101. According to the adsorption isotherm classification, the adsorption-desorption isotherm of etched MIL-101 belongs to the Langmuir adsorption isotherm, which indicates that the etching processes does not change the isothermal adsorption type of the MIL-101.

3.2. Iodine Adsorption Study. To study the effect of the etching time on the adsorption properties of sample for gaseous iodine, the capture experiment of gaseous iodine was completed and the experimental results are shown in Figure 6. The saturation adsorption capacity of etching 1 h of MIL-101 was 298 wt%, it is close to that of the MIL-101. The saturation adsorption capacity of MIL-101 with etching times of 3 h, 4 h, and 6 h were 352 wt%, 371 wt%, and 337 wt%, respectively, which were higher than that of the MIL-101 to gaseous iodine. It is clearly found that the saturation adsorption capacity of etched MIL-101 for gaseous iodine has increases firstly and decreases afterwards with the increasing etching time. When the MIL-101 with etching times of 4 h reaches maximum, the value is about 371 wt%. The saturation adsorption capacity of MIL-101 with 4 h etching times is 1.23 times compared to that of MIL-101 for gaseous iodine. The experimental results indicated that adjusting the MIL-101 pore structure by etching process can improve the adsorption performance of MIL-101 for gaseous iodine, although etching process reduced the specific area of the material. The reason is that the benzene ring is exposed, and it can provide more adsorption sites.

Because of the optimal adsorption performance, MIL-101 with 4 h etching was chosen to study the adsorption capacity for different initial masses of iodine. The results are shown in Figure 7(a). The adsorption capacity of absorber for gaseous iodine increases rapidly with the initial mass of iodine, and the saturation adsorption capacity reach maximal value at 300 mg. The saturated adsorption point of etched MIL-101 (4 h) was reduced from 400 mg of MIL-101 to 300 mg. The experimental results indicate that the increasing pore volume improved the adsorption performance for low concentration iodine.

In order to research the adsorption rate of etched MIL-101 for gaseous iodine, the adsorption kinetics of etched MIL-101 was tested at 75°C and environmental pressure. The adsorption rate for iodine is fast within the first 4 hours, but the rate is decreased in the following time. The adsorption capacity reaches its limit after 8 h as shown in Figure 7(b). The main reason is the more adsorption sites were provided, the less iodine molecule was adsorbed. However, as the adsorption site is fully occupied, the adsorption driving force gradually weakens until it completely disappears. The higher adsorption capacity indicates that the special structure after etching could have provided more space to accommodate iodine. Table 2 summarizes some of these adsorption values reported in the literature.

Before and after iodine adsorption, X-ray photoelectric spectroscopy (XPS) was measured to research adsorption mechanism, and the results are shown in Figure 8(a). As

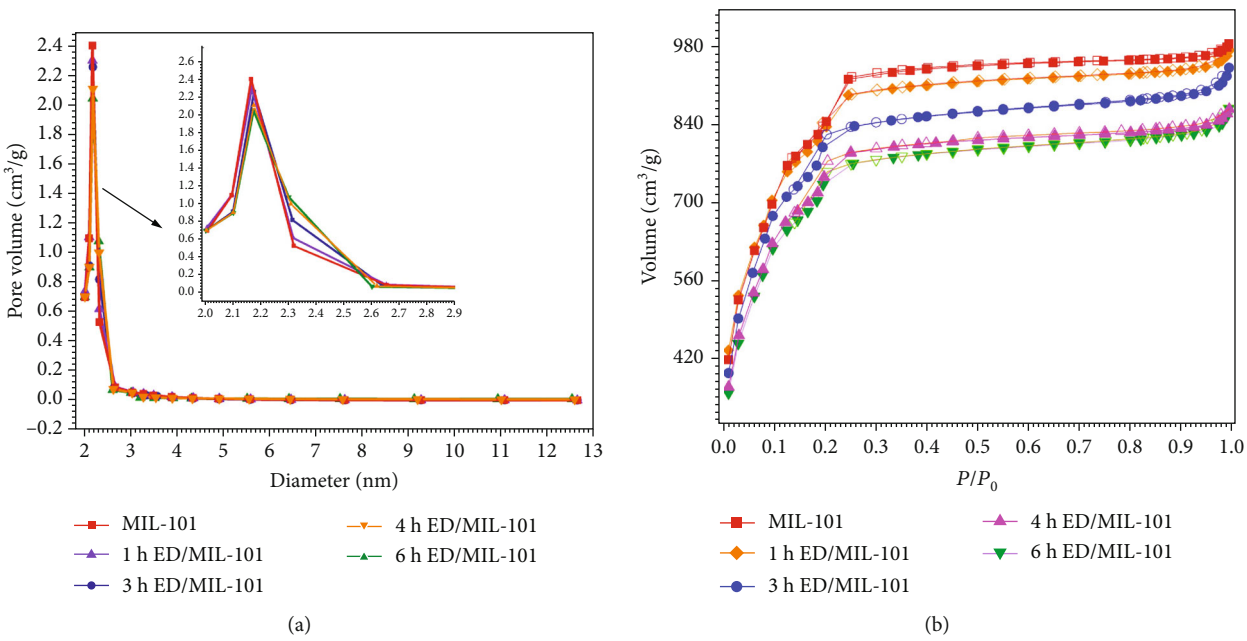

Figure 5: (a) The curves of aperture distribution; (b) nitrogen adsorption-desorption isotherms of etched MIL-101.

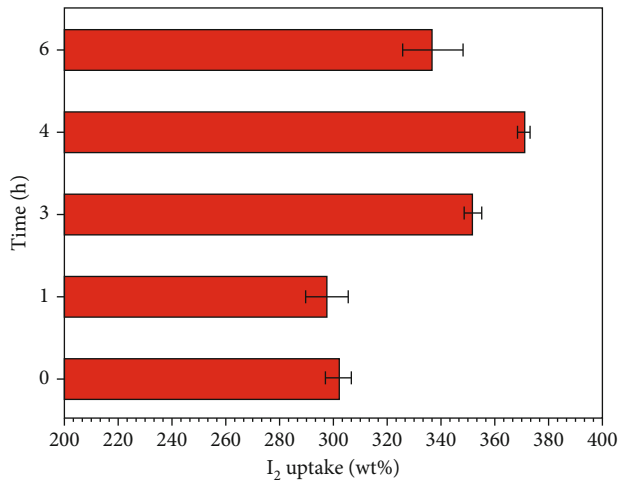

Figure 6: Saturation adsorption capacity of MIL-101 with different etching times for gaseous iodine.

shown in Figure 8(a), the spectrum XPS was used to analyze the state of the constituent elements after iodine adsorption and it was corrected by C-1 s (284.8 eV). The etched MIL-101 and MIL-101 contained elements, such as C, N, O, and Cr. After iodine adsorption, I_2 peaks appeared at 631.3 eV and 619.8 eV in the XPS spectrum of etched MIL-101 [41, 42]. Combining with Figure 8(b), it is determined that the surface adsorbed iodine of valence is zero. That is to say that the iodine adsorption of etched MIL-101 belongs to physical adsorption.

After I_2 adsorption, the XRD spectrum of etched MIL-101 is shown in Figure 9(a). It can be observed from Figure 9 that the position of the characteristic peak of etched MIL-101 does not change and the strength of the characteristic peak is weakened, before and after adsorption. This result showed that the crystal structure was still maintained. Figure 9(b) is the FT-IR spectrum of the etched MIL-101 after adsorption iodine. Comparing FT-IR spectrum before and after adsorption, no new characteristic peaks were observed, indicating that the structure of etched MIL-101 does not change after adsorption, in other words, I_2 does not react with the etched MIL-101, it is just being adsorbed onto the surface and pore through static electricity action.

3.3. Adsorption Mechanism Analysis. The reason that the etching process improves the adsorption capacity needs to be studied. Based on previous research results, the specific surface area is the major factor for adsorption capacity. The larger the specific surface area is, the bigger the area contacted with the gaseous is. The specific surface areas of etched MIL-101 are 3134 m^2/g (0 h etching time), 3071 m^2/g (1 h etching time), 2902 m^2/g (3 h etching time), 2753 m^2/g (4 h etching time), and 2524 m^2/g (6 h etching time), respectively. According to the specific surface area, the etching process should reduce iodine adsorption properties. In order to seek the reasons, the adsorption capacity per unit specific surface area is defined. It represents the utilization efficiency per unit specific surface and the calculation equation is shown as follows:

$$\varepsilon = \frac{m}{s}, \tag{2}$$

where ε is the adsorption capacity per unit specific surface area (wt%•g/m^2), m is the mass of adsorption amount of iodine (wt%), and s is the specific surface area (m^2/g). The absorption capacity of iodine unit surface area corresponds to 0.096 wt%·g/m^2 (0 h etched MIL-101), 0.097 wt%·g/m^2 (1 h etched MIL-101), 0.127 wt%•g/m^2 (3 h etched MIL-101), 0.135 wt%·g/m^2 (4 h etched MIL-101), and 0.134 wt%·g/m^2 (6 h etched MIL-101), respectively. As can be seen from the

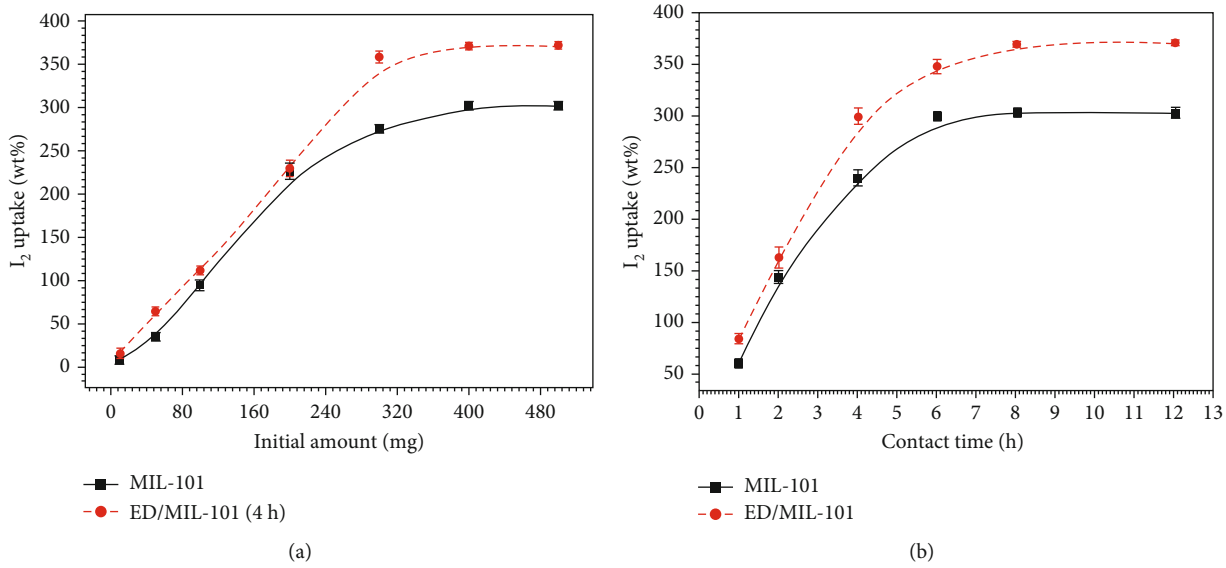

Figure 7: (a) The adsorption capacity of etched MIL-101 (4 h) for different initial mass of iodine. (b) The adsorption kinetics of etched MIL-101(4 h) and MIL-101.

Table 2: Comparison of iodine adsorption capacities of as-prepared etched MIL-101(4 h) with other adsorbents reported in the literature.

Adsorbent	Equilibration time (h)	Adsorption capacity (mg/g)	Specific surface area (m^2/g)	Reference
Ag°-mordenite zeolite	130	110	109	[36]
SCMP-2	5	2220	855	[37]
ZIF-8	12	1250	2 643	[21]
Cu-BTC	12	1750	1850	[38]
MFM-300	12	1540	1250	[39]
ZIF-L	6	2637	1922	[40]
QTD-COF-1	10	4620	—	[11]
TTMDATA	20	4490	456	[10]
Etched MIL-101(4 h)	8	3710	2753	This work

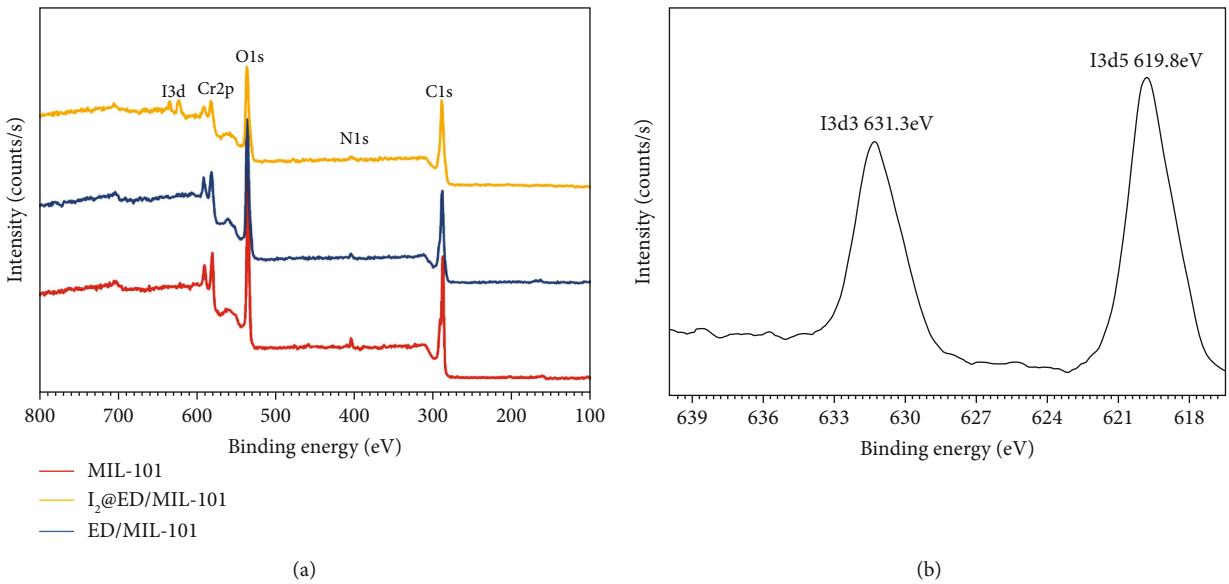

Figure 8: X-ray photoelectric spectroscopy. (a) Full energy spectrum. (b) Local energy spectrum.

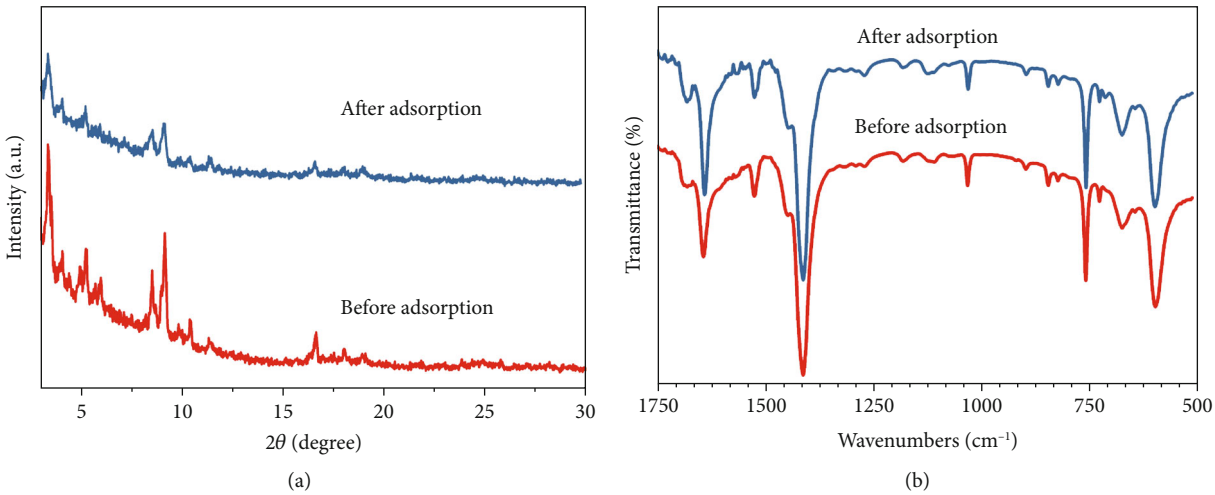

Figure 9: (a) The XRD spectrum of etched MIL-101 after adsorption iodine. (b) The FT-IR spectrum of the etched MIL-101 after adsorption iodine.

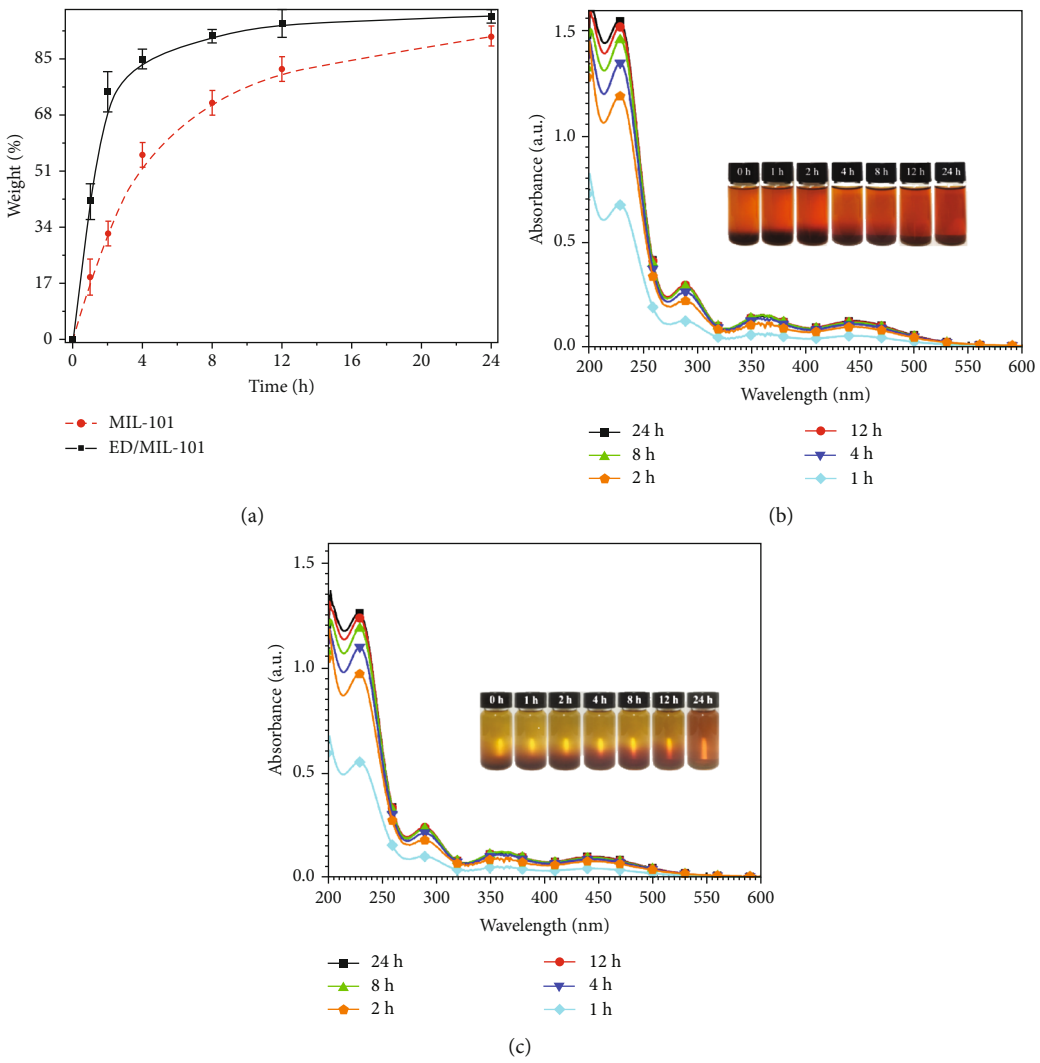

Figure 10: (a) The iodine release rate of etched MIL-101 and MIL-101 in ethanol. (b) The absorbance curve of solutions with different iodine release time for etched MIL-101. (c) The absorbance curve of solutions with different iodine release time for MIL-101.

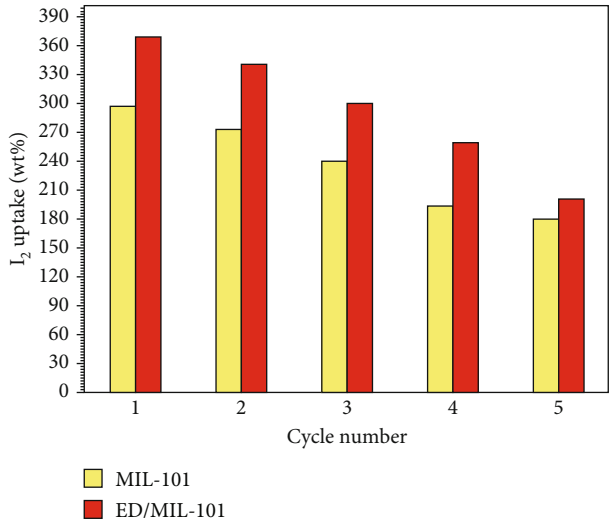

Figure 11: The circulating performance of etched MIL-101 and MIL-101.

results, the absorption capacity unit surface area of 4 h etched MIL-101 is the highest. Compared with 3 h etched MIL-101, the total absorption amount of 6 h etched MIL-101 is worse. However, the absorption capacity unit surface area of 6 h etched MIL-101 is better than that of 3 h etched MIL-101. The adsorption type is not changed, the material structure is not changed, and no other material is added. The etching process may be able to increase some adsorption sites [43]. However, 1 h or 3 h of etching is not optimal. The reason is that there are other factors besides the adsorption site. From the experimental results, that is, the roughness of the inner surface of the pore and previous research also confirms the conclusion. There is a threshold for the roughness influence, and the roughness will significantly improve the adsorption capacity in a range. The results of SEM indicated that the roughness of surface is increased.

The similar results also appear in the Cu nanoparticles doped MIL-101, the previous study in our group needs to be cited, Cu/MIL-101 was successfully synthesized for highly efficient capture of iodine [44]. The Cu nanoparticles is attached to the surface of pore, as the copper content gradually increases, more particles are deposited on the surface pore. The absorption capacity unit surface area of Cu/MIL-101 corresponds to 0.096 wt%•g/m^2 (0 wt% Cu/MIL-101), 0.103 wt%•g/m^2 (0.5 wt% Cu/MIL-101), 0.151 wt%•g/m^2(1 wt% Cu/MIL-101), and 0.143 wt%•g/m^2 (2 wt% Cu/MIL-101), respectively. The specific surface areas of Cu/MIL-101 are 3134 m^2/g (0 wt% Cu/MIL-101), 2802 m^2/g (0.5 wt% Cu/MIL-101), 2264 m^2/g (1 wt% Cu/MIL-101), and 1975 m^2/g (2 wt% Cu/MIL-101). The general change of specific surface areas also has been down. It indicates that some of the pores are blocked by Cu particles. Compared with MIL-101, all kinds of Cu/MIL-101 have stronger adsorption capacity. The main reason is that nanoparticles increase the absorption site and these Cu particles lead to the pore of MIL-101 become rough. If it is simply an increase in active sites, the 0.5 wt% Cu/MIL-101 has improved adsorption efficiency by 7%, compared with the 1 wt% Cu/MIL-101, the adsorption efficiency has risen by 57%. Therefore, the surface roughness also significantly improves the adsorption capacity in a range. The 1 wt%Cu/MIL-101 is optimal in all aspects of the pore roughness, adsorption site, and specific surface area.

3.4. Adsorption Circulating Performance. The adsorbed samples were sunk in ethanol to release the adsorbed iodine. As shown in Figure 10, the ethanol color gradually became dark brown after releasing iodine. It indicates that the iodine solved into ethanol from etched MIL-101. Compared with MIL-101, the etched MIL-101 can release more iodine and the solution is also dark-colored, as shown in Figures 10(b) and 10(c). The absorbance curves of solutions with different iodine release time are used to assess the iodine concentration. The iodine rapidly released from the etched MIL-101 as time goes on, and the release rate can reach 75% at 2 h, about 85% at 4 h, about 92% at 8 h, about 96% at 12 h, and about 98% at 24 h, as shown in Figure 10(a). The iodine releasing rate of etched MIL-101 is more quick than that of MIL-101. The reason is that the etching process makes the material pore size bigger, and the solvent is easier to enter [45, 46]. There is a huge gap for the amount of iodine released in the first eight hours. The etched MIL-101 just needs to be released for eight hours to achieve satisfactory results. The results prove that the etched MIL-101 is recyclable within three cycles and that is a very important property in practical application, and the adsorbent can be used again in an emergency.

In order to explore the circulating performance of etched MIL-101, the adsorption circulating experiment of iodine was accomplished. After disattachment, the gaseous iodine was readsorbed according to the adsorption experiment, and the results are shown in Figure 11. The etched MIL-101 maintained 92% adsorption performance after the second cycle, 81% after the third cycle, and 54% after five cycles. It can be known from the measurement results that circulating performance of etched MIL-101 is consistent with that of MIL-101, and the etching MIL-101 has excellent adsorption performance within three cycles.

4. Conclusions

The MIL-101 was prepared by hydrothermal synthesis, and then the etched MIL-101 was generated successfully by glacial acetic acid etching. The etching process reduces the specific surface area, but it increases the adsorption capacity for gaseous iodine. The SEM and TEM results of etched MIL-101 show that material morphology remains unchanged, but its crystal surface and pore inner surface became rough. The curves of XRD, FT-IR, and XPS indicate that the crystal structure and material composition does not any change. The results of this experiment and previous related experiments were analyzed. The roughness is also an important factor for adsorption capacity. The roughness, adsorption site, and specific surface area can affect the adsorption properties of adsorbent, and the application process can be optimized through these three aspects. When MOF materials are treated by etching process, it is necessary to optimize the

etching time through preexperiment before application. Compared with adsorption capacity of MIL-101(302 wt%), the optimal etching time is 4 h, and the saturated adsorption capacity of etched MIL-101 (4 h) is 371 wt%. The results show that the adsorption capacity has risen by 22%. In addition, the adsorbed I_2 does not react with adsorbent and the adsorption process belongs to physical adsorption. Therefore, the adsorbent can be reused through iodine release. The method of desorption is ethanol washing and evaporation drying. The iodine cycle experiment shows that the etched MIL-101 has good cycle performance within three times. The etched MIL-101 has advantages of simple preparation method, low cost, high absorption capacity, and recyclable utilization. In the future, the adsorbent can be used within eight hours of a nuclear accident emergency, such as the adsorption layer of the mask and enrichment material for radioactive iodine activity monitoring.

Data Availability

The data used to support the findings of this study are available from the corresponding author upon request.

Conflicts of Interest

The authors declare that they have no conflicts of interest.

Acknowledgments

The present work was supported by the National Natural Science Foundation of China (Grant No. 11905106), the Natural Science Foundation of Jiangsu Province (Grant No. BK20190410), the Chinese Postdoctoral Science Foundation (Grant No. 2022 M711631), and the Fundamental Research Funds for the Central Universities (Grant No. NJ2022019-2).

References

[1] Y.-Y. Han, A. O. Youk, H. Sasser, and E. O. Talbott, "Cancer incidence among residents of the Three Mile Island accident area: 1982-1995," *Environmental Research*, vol. 111, no. 8, pp. 1230–1235, 2011.

[2] F. Kepak, "Removal of gaseous fission products by adsorption," *Journal of Radioanalytical and Nuclear Chemistry*, vol. 142, no. 1, pp. 215–230, 1990.

[3] V. Hansen, P. Yi, X. Hou, A. Aldahan, P. Roos, and G. Possnert, "Iodide and iodate (129I and 127I) in surface water of the Baltic Sea, Kattegat and Skagerrak," *Science of the Total Environment*, vol. 412-413, pp. 296–303, 2011.

[4] C. Pei, T. Ben, S. Xu, and S. Qiu, "Ultrahigh iodine adsorption in porous organic frameworks," *Journal of Materials Chemistry A*, vol. 2, no. 20, pp. 7179–7187, 2014.

[5] C. Falaise, C. Volkringer, J. Facqueur, T. Bousquet, L. Gasnot, and T. Loiseau, "Capture of iodine in highly stable metal–organic frameworks: a systematic study," *Chemical Communications*, vol. 49, no. 87, pp. 10320–10322, 2013.

[6] J. Wang, J. Luo, X. Luo et al., "Assembly of a three-dimensional metal–organic framework with copper (I) iodide and 4-(pyrimidin-5-yl) benzoic acid: controlled uptake and release of iodine," *Crystal Growth & Design*, vol. 15, no. 2, pp. 915–920, 2015.

[7] R. E. Morris and P. S. Wheatley, "Gas storage in nanoporous materials," *Angewandte Chemie International Edition*, vol. 47, no. 27, pp. 4966–4981, 2008.

[8] K. W. Chapman, P. J. Chupas, and T. M. Nenoff, "Radioactive iodine capture in silver-containing mordenites through nanoscale silver iodide formation," *Journal of the American Chemical Society*, vol. 132, no. 26, pp. 8897–8899, 2010.

[9] F. J. Herrmann, B. Herrmann, and V. Hoeflich, "Removal efficiency of silver impregnated filter materials and performance of iodie filters in the off-gas of the Karlsruhe reprocessing plant WAK," in *Proceedings of the 24. DOE/NRC nuclear air cleaning and treatment*, Harvard Univ., Boston, MA, 1997.

[10] T. Geng, W. Zhang, Z. Zhu, and X. Kai, "Triazine-based conjugated microporous polymers constructing triphenylamine and its derivatives with nitrogen as core for iodine adsorption and fluorescence sensing I_2," *Microporous and Mesoporous Materials*, vol. 273, pp. 163–170, 2019.

[11] X. Guo, Y. Li, M. Zhang et al., "Colyliform crystalline 2D covalent organic frameworks (COFs) with quasi-3D topologies for rapid I2 adsorption," *Angewandte Chemie International Edition*, vol. 59, no. 50, pp. 22697–22705, 2020.

[12] S. Wang, J. Cui, S. Zhang, X. Xie, and W. Xia, "Enhancement thermal stability and CO2adsorption property of ZIF-8 by pre-modification with polyaniline," *Materials Research Express*, vol. 7, no. 2, article 025304, 2020.

[13] J. Khan, N. Iqbal, A. Asghar, and T. Noor, "Novel amine functionalized metal organic framework synthesis for enhanced carbon dioxide capture," *Materials Research Express*, vol. 6, no. 10, article 105539, 2019.

[14] Y. Feng, P. Yang, Y. Li, and J. Gu, "AgNPs-containing metal–organic frameworks for the effective adsorption and immobilization of radioactive iodine," *Journal of Chemical & Engineering Data*, vol. 65, no. 4, pp. 1986–1992, 2020.

[15] K. M. Qasem, S. Khan, M. N. Ahamad, H. A. Saleh, M. Ahmad, and M. Shahid, "Radioactive iodine capture by metal organic frameworks in liquid and vapour phases: an experimental, kinetic and mechanistic study," *Journal of Environmental Chemical Engineering*, vol. 9, no. 6, article 106720, 2021.

[16] W. W. Xu, S. Pramanik, Z. Zhang, T. J. Emge, and J. Li, "Microporous metal organic framework [M2 (hfipbb) 2 (ted)](M= Zn, co; H2hfipbb=4, 4-(hexafluoroisopropylidene)-bis (benzoic acid); ted= triethylenediamine): synthesis, structure analysis, pore characterization, small gas adsorption and CO2/N2 separation properties," *Journal of Solid State Chemistry*, vol. 200, pp. 1–6, 2013.

[17] X. Zhao, B. Xiao, A. J. Fletcher, K. M. Thomas, D. Bradshaw, and M. J. Rosseinsky, "Hysteretic adsorption and desorption of hydrogen by nanoporous metal-organic frameworks," *Science*, vol. 306, no. 5698, pp. 1012–1015, 2004.

[18] H.-H. Wang, L.-N. Jia, L. Hou, W.-j. Shi, Z. Zhu, and Y.-Y. Wang, "A new porous MOF with two uncommon metal–carboxylate–pyrazolate clusters and high CO2/N2 selectivity," *Inorganic Chemistry*, vol. 54, no. 4, pp. 1841–1846, 2015.

[19] H. G. T. Nguyen, N. M. Schweitzer, C.-Y. Chang et al., "Vanadium-node-functionalized UiO-66: a thermally stable MOF-supported catalyst for the gas-phase oxidative dehydrogenation of cyclohexene," *ACS Catalysis*, vol. 4, no. 8, pp. 2496–2500, 2014.

[20] R. J. Kuppler, D. J. Timmons, Q.-R. Fang et al., "Potential applications of metal-organic frameworks," *Coordination Chemistry Reviews*, vol. 253, no. 23-24, pp. 3042–3066, 2009.

[21] D. F. Sava, M. A. Rodriguez, K. W. Chapman et al., "Capture of volatile iodine, a gaseous fission product, by zeolitic imidazolate framework-8," *Journal of the American Chemical Society*, vol. 133, no. 32, pp. 12398–12401, 2011.

[22] K. W. Chapman, D. F. Sava, G. J. Halder, P. J. Chupas, and T. M. Nenoff, "Trapping guests within a nanoporous metal–organic framework through pressure-induced amorphization," *Journal of the American Chemical Society*, vol. 133, no. 46, pp. 18583–18585, 2011.

[23] G. Férey, C. Mellot-Draznieks, C. Serre et al., "A chromium terephthalate-based solid with unusually large pore volumes and surface area," *Science*, vol. 309, no. 5743, pp. 2040–2042, 2005.

[24] Y. Chen, P. Mao, X. Yin, Y. Yang, X. Yan, and L. U. Jiaqi, "Preparation of Ag doped MIL-101 and its adsorption performance for iodide ions," China Powder Science and Technology, 2016.

[25] I. Ahmed, N. A. Khan, and S. H. Jhung, "Graphite oxide/metal–organic framework (MIL-101): remarkable performance in the adsorptive denitrogenation of model fuels," *Inorganic Chemistry*, vol. 52, no. 24, pp. 14155–14161, 2013.

[26] Z. Zhou, L. Mei, C. Ma et al., "A novel bimetallic MIL-101(Cr, Mg) with high CO2 adsorption capacity and CO2/N2 selectivity," *Chemical Engineering Science*, vol. 147, pp. 109–117, 2016.

[27] M. Montazerolghaem, S. F. Aghamiri, S. Tangestaninejad, and M. R. Talaie, "A metal–organic framework MIL-101 doped with metal nanoparticles (Ni & Cu) and its effect on CO2adsorption properties," *RSC Advances*, vol. 6, no. 1, pp. 632–640, 2016.

[28] E. A. Berdonosova, K. A. Kovalenko, E. V. Polyakova, S. N. Klyamkin, and V. P. Fedin, "Influence of anion composition on gas sorption features of Cr-MIL-101 metal–organic framework," *The Journal of Physical Chemistry C*, vol. 119, no. 23, pp. 13098–13104, 2015.

[29] P. D. Du, H. T. M. Thanh, Thuy Chau To et al., "Metal-organic framework MIL-101: synthesis and photocatalytic degradation of remazol black B dye," *Journal of Nanomaterials*, vol. 2019, Article ID 6061275, 15 pages, 2019.

[30] W. Liu, J. Huang, Q. Yang et al., "Multi-shelled hollow metal–organic frameworks," *Angewandte Chemie International Edition*, vol. 56, no. 20, pp. 5512–5516, 2017.

[31] D. Banerjee, X. Chen, S. Lobanov et al., "Iodine adsorption in metal organic frameworks in the presence of humidity," *ACS Applied Materials & Interfaces*, vol. 10, no. 13, pp. 10622–10626, 2018.

[32] M. Anbia and V. Hoseini, "Enhancement of CO2 adsorption on nanoporous chromium terephthalate (MIL-101) by amine modification," *Journal of Natural Gas Chemistry*, vol. 21, no. 3, pp. 339–343, 2012.

[33] L. Bromberg, Y. Diao, H. Wu, S. A. Speakman, and T. A. Hatton, "Chromium(III) terephthalate metal organic framework (MIL-101): HF-free synthesis, structure, polyoxometalate composites, and catalytic properties," *Chemistry of Materials*, vol. 24, no. 9, pp. 1664–1675, 2012.

[34] M. H. Choi, S. W. Jeong, H. E. Shim et al., "Efficient bioremediation of radioactive iodine using biogenic gold nanomaterial-containing radiation-resistant bacterium, Deinococcus radiodurans R1," *Chemical Communications*, vol. 53, no. 28, pp. 3937–3940, 2017.

[35] C. Yan and T. Mu, "Investigation of ionic liquids for efficient removal and reliable storage of radioactive iodine: a halogen-bonding case," *Physical Chemistry Chemical Physics*, vol. 16, no. 11, pp. 5071–5075, 2014.

[36] T. M. Nenoff, M. A. Rodriguez, N. R. Soelberg, and K. W. Chapman, "Silver-mordenite for radiologic gas capture from complex streams: dual catalytic CH3I decomposition and I confinement," *Microporous and Mesoporous Materials*, vol. 200, pp. 297–303, 2014.

[37] X. Qian, Z.-Q. Zhu, H.-X. Sun et al., "Capture and reversible storage of volatile iodine by novel conjugated microporous polymers containing Thiophene units," *ACS Applied Materials & Interfaces*, vol. 8, no. 32, pp. 21063–21069, 2016.

[38] D. F. Sava, K. W. Chapman, M. A. Rodriguez et al., "Competitive I2 sorption by Cu-BTC from humid gas streams," *Chemistry of Materials*, vol. 25, no. 13, pp. 2591–2596, 2013.

[39] X. Zhang, I. Da Silva, H. G. Godfrey et al., "Confinement of iodine molecules into triple-helical chains within robust metal–organic frameworks," *Journal of the American Chemical Society*, vol. 139, no. 45, pp. 16289–16296, 2017.

[40] H. Xiao, H. Zhou, S. Feng, D. B. Gore, Z. Zhong, and W. Xing, "In situ growth of two-dimensional ZIF-L nanoflakes on ceramic membrane for efficient removal of iodine," *Journal of Membrane Science*, vol. 619, article 118782, 2021.

[41] Z. Yan, Y. Yuan, Y. Tian, D. Zhang, and G. Zhu, "Highly efficient enrichment of volatile iodine by charged porous aromatic frameworks with three sorption sites," *Angewandte Chemie*, vol. 127, no. 43, pp. 12924–12928, 2015.

[42] T. Jing-Juan, Y. Ming-Lu, M. Yun, L. Shi-Jun, and G. Ze-Hong, "Removal of radioiodine from nuclear-fuel-reprocessing off-gases with silver-nitrate-impregnated silica gel," *Journal of Radioanalytical and Nuclear Chemistry*, vol. 119, no. 2, pp. 109–118, 1987.

[43] P. Y. Cheng, D. Zhong, and A. H. Zewail, "Microscopic solvation and femtochemistry of charge-transfer reactions: the problem of benzene(s)-iodine binary complexes and their solvent structures," *Chemical Physics Letters*, vol. 242, no. 4-5, pp. 369–379, 1995.

[44] B. Qi, Y. Liu, T. Zheng et al., "Highly efficient capture of iodine by Cu/MIL-101," *Journal of Solid State Chemistry*, vol. 258, pp. 49–55, 2018.

[45] Y. Zhou, M. Jia, X. Zhang, and J. Yao, "Etched ZIF-8 as a filler in mixed-matrix membranes for enhanced CO2/N2Separation," *Chemistry – A European Journal*, vol. 26, no. 35, pp. 7918–7922, 2020.

[46] Y. Feng and J. Yao, "Tailoring the structure and function of metal organic framework by chemical etching for diverse applications," *Coordination Chemistry Reviews*, vol. 470, article 214699, 2022.